

Rabi oscillations in a quantum dot-cavity system coupled to a non-zero temperature phonon bath

Jonas Larson¹ and Héctor Moya-Cessa²

¹ICFO-Institut de Ciències Fotòniques, E-08860 Castelldefels, Barcelona, Spain

²INAOE, Coordinación de Óptica, Apdo. Postal 51 y 216, 72000 Puebla, Pue., Mexico

(Dated: January 24, 2020)

We study a quantum dot strongly coupled to a single high-finesse optical microcavity mode. We use a rotating wave approximation method, commonly used in ion-laser interactions, to obtain an analytic solution of this problem beyond the Born-Markov approximation. The decay of Rabi oscillations because of the electron-phonon coupling are studied at arbitrary temperature and analytical expressions for the collapse and revival times are presented. Analysis without the rotating wave approximation are presented by means of investigating the energy spectrum.

PACS numbers:

I. INTRODUCTION

Semiconductor quantum dots (QD) have emerged as promising candidates for studying quantum optical phenomena [1]. In particular, cavity quantum electrodynamics (CQED) effects can be investigated using a single QD embedded inside a photonic nano-structure [2]. One of the most fundamental systems in CQED is an atom interacting with a quantized field [3], such a system has been an invaluable tool to understand quantum phenomena [4] as well as for considerations on its applications to realize quantum information [5]. Similar systems (in the sense of their treatment, applications, etc.) like trapped ions interacting with lasers [6] have shown to be an alternative to develop techniques for quantum information processing [7] and the study of fundamental effects [8]. Recent developments in semiconductor nano-technology have shown that excitons in QD constitute yet another two-level system for CQED effects [9]. Contrary to the atom-field interaction where dissipative effects can be fairly overlooked provided the coupling strength between atom and field is sufficiently large compared to the dissipation rate due to cavity losses, the physics of a quantum dot microcavity is enriched by the presence of electro-electron and electron-phonon interactions, indicating that decoherence due to phonons may imply fundamental limitations to quantum information processing on quantum dot CQED [10]. Here, we would like to analyze the effects of electron-phonon interactions on electron-hole-photon Rabi oscillations in cavity QED.

As in Ref. [11, 12], we will not apply the Born-Markov approximation [13], but will use a different technique for solving this problem. In particular we will make use of techniques commonly applied in ion-laser interactions. It relies on the rotating wave approximation RWA, and within this approximation the Hamiltonian becomes diagonal with respect to the phonon subsystem, which is shown in sec. II. In the validity regime of the RWA, the decoherence effect on the inversion, due to the phonon bath, is analyzed in sec. III. Further approximations, valid in large parameter ranges, are introduced in order

to achieve analytical expressions for the collapse and revival times. The zero temperature situation has been investigated in [12], while here we study the effects due to zero as well as non-zero temperatures (causing the collapse of the revivals), and also how different phonon mode structures affect the decoherence. A different method to treat the non-zero temperature case was discussed in [14], where the collapse time is obtained numerically. The dynamics beyond the rotating wave approximation, shortly studied here in sec. IV, becomes highly complex as can be seen from the energy spectrum. How the phonon decoherence could be used as a possible resource for various applications is briefly mentioned in the concluding remarks.

II. THE MODEL

We assume a simple two-level model for the electronic degrees of freedom of the QD, consisting of the QD electronic ground state, $|g\rangle$, and the lowest energy electron-hole (exciton) state, $|e\rangle$, with the Hamiltonian [11] ($\hbar = 1$)

$$\hat{H} = \omega_{eg}\hat{\sigma}_{ee} + \omega\hat{a}^\dagger\hat{a} + g(\hat{a}^\dagger\hat{\sigma}_- + \hat{\sigma}_+\hat{a}) + \hat{\sigma}_{ee}\sum_k \lambda_k(\hat{b}_k^\dagger + \hat{b}_k) + \sum_k \omega_k \hat{b}_k^\dagger \hat{b}_k, \quad (1)$$

where $\hat{\sigma}_+ = |e\rangle\langle g|$, \hat{a} and \hat{b}_k are the annihilation operators for the cavity mode and the k th phonon mode, respectively. By transforming to a rotating frame, with frequency ω

$$\hat{\mathcal{H}} = \Delta\hat{\sigma}_{ee} + g(\hat{a}^\dagger\hat{\sigma}_- + \hat{\sigma}_+\hat{a}) + \hat{\sigma}_{ee}\sum_k \lambda_k(\hat{b}_k^\dagger + \hat{b}_k) + \sum_k \omega_k \hat{b}_k^\dagger \hat{b}_k \quad (2)$$

where $\Delta = \omega_{eg} - \omega$ is the detuning. Now we use the transformation [10, 15]

$$\hat{T} = \prod_k e^{\hat{\sigma}_{ee} \frac{\lambda_k}{\omega_k} (\hat{b}_k^\dagger - \hat{b}_k)} \quad (3)$$

to obtain the Hamiltonian $\hat{\mathcal{H}}_T = \hat{T}\hat{\mathcal{H}}\hat{T}^\dagger$

$$\begin{aligned}\hat{\mathcal{H}}_T &= (\Delta - \Delta_\eta) \hat{\sigma}_{ee} + \sum_k \omega_k \hat{b}_k^\dagger \hat{b}_k \\ &+ g \left[\hat{a}^\dagger \hat{\sigma}_- \prod_k \hat{D}_b(\eta_k) + \hat{\sigma}_+ \hat{a} \prod_k \hat{D}_b^\dagger(\eta_k) \right],\end{aligned}\quad (4)$$

with $\eta_k = \lambda_k/\omega_k$, $\Delta_\eta = \sum_k \omega_k \eta_k^2$ is the so-called polaron shift [15] and $\hat{D}_b(\eta_k) = \exp(\eta_k \hat{b}^\dagger - \eta_k^* \hat{b})$. For simplicity we look at the case $\Delta = \Delta_\eta$ to obtain

$$\hat{\mathcal{H}}_T = g \left[\hat{a}^\dagger \hat{\sigma}_- \prod_k \hat{D}_b(\eta_k) + \hat{\sigma}_+ \hat{a} \prod_k \hat{D}_b^\dagger(\eta_k) \right] + \sum_k \omega_k \hat{b}_k^\dagger \hat{b}_k. \quad (5)$$

Now by transforming to an interaction picture

$$\hat{H}_I = g \left[\hat{a}^\dagger \hat{\sigma}_- \prod_k \hat{D}_b(\eta_k e^{-i\omega_k t}) + \hat{\sigma}_+ \hat{a} \prod_k \hat{D}_b^\dagger(\eta_k e^{-i\omega_k t}) \right] \quad (6)$$

and applying the rotating wave approximation in the above equation, the final Hamiltonian is obtained:

$$\hat{H}_{rwa} = \tilde{g} \left[\hat{a}^\dagger \hat{\sigma}_- \prod_k L_{\hat{n}_k}(\eta_k^2) + \hat{\sigma}_+ \hat{a} \prod_k L_{\hat{n}_k}(\eta_k^2) \right] \quad (7)$$

where $L_{\hat{n}_k}$ are the Laguerre polynomials of order \hat{n}_k [16, 17] and $\tilde{g} = g \exp(\xi/2) \equiv g \exp(-\sum_k \eta_k^2/2)$ is a rescaled Rabi vacuum frequency. The parameter ξ is sometimes referred to as the Huang-Rhys factor [18], and it is usually very small, $\xi \ll 1$, [19, 20] but it can become much larger, $\xi \sim 1$, [21]. The above equation is readily solvable, finding the evolution operator as

$$\hat{U} = \hat{U}_{ee} \hat{\sigma}_{ee} + \hat{U}_{gg} \hat{\sigma}_{gg} + \hat{U}_{eg} \hat{\sigma}_- + \hat{U}_{ge} \hat{\sigma}_+, \quad (8)$$

where

$$\hat{U}_{ee}(t; \hat{n}) = \cos \hat{\Omega}_{k, \hat{n}+1} t, \quad (9)$$

$$\hat{U}_{ge}(t; \hat{n}) = -i\epsilon \hat{a} \frac{\sin \hat{\Omega}_{k, \hat{n}} t}{\hat{\Omega}_{k, \hat{n}}}, \quad (10)$$

$$\hat{U}_{eg}(t; \hat{n}) = -i\epsilon \hat{a}^\dagger \frac{\sin \hat{\Omega}_{k, \hat{n}+1} t}{\hat{\Omega}_{k, \hat{n}+1}}, \quad (11)$$

and

$$\hat{U}_{gg}(t; \hat{n}) = \cos \hat{\Omega}_{k, \hat{n}} t, \quad (12)$$

with

$$\hat{\Omega}_{\hat{n}} = \hat{\epsilon} \sqrt{\hat{n}} = \tilde{g} L_{\hat{n}_k}(\eta_k^2) \sqrt{\hat{n}}. \quad (13)$$

III. DYNAMICS

Having the evolution operator, we can in principle calculate any properties we want, in particular we look at the Rabi oscillations for the two-levels system, which has been studied experimentally in quantum dot systems [20]. By means of the inversion operator $\sigma_z = |e\rangle\langle e| - |g\rangle\langle g|$

$$W(t) = \text{Tr}\{\rho(t)\sigma_z\} \quad (14)$$

where $\rho(t) = \hat{U}\rho(0)\hat{U}^\dagger$ and $\rho(0)$ is the initial density matrix, Rabi oscillations will be analyzed. This initial state is chosen as the fully separable state

$$\rho(0) = \prod_k \rho_k(0) |0, e\rangle\langle 0, e| \quad (15)$$

with the atom excited, the cavity mode in vacuum and the phonon modes are all assumed to be in a thermal distribution

$$\rho_k(0) = \sum_{n_k=0}^{\infty} |c_{n_k}|^2 |n_k\rangle\langle n_k| = \sum_{n_k=0}^{\infty} \frac{\bar{n}_k^{n_k}}{(\bar{n}_k + 1)^{n_k+1}} |n_k\rangle\langle n_k|. \quad (16)$$

The inversion can be written explicitly as

$$W(t) = \sum_{\{n_k\}} \prod_k |c_{n_k}|^2 \cos \left(2\tilde{g} \prod_{k'} L_{n_{k'}}(\eta_{k'}^2) t \right), \quad (17)$$

where the summation goes from 0 to ∞ and runs over all modes. For $t = 0$ we have $W(0) = 1$ as expected, while for $t \neq 0$ the sum will in general differ from 1. Interestingly we note that at zero temperature, $T = 0$, $|c_{n_k}| = \delta_{n_k, 0}$ for all k and thus, at absolute zero temperature the system Rabi oscillations are intact but with a rescaled frequency [12]. Because the argument of the cosine function consists of a product of functions with different mode indices k , the expression can in general not be separated. Nonetheless, under some assumptions the inversion (17) can be greatly simplified. As mentioned in the previous section, usually $\eta \ll 1$ and we may expand the Laguerre polynomials

$$L_n(\eta^2) = \sum_{m=0}^n \binom{n}{m} \frac{\eta^{2m}}{m!} = 1 - n\eta^2 + \frac{n(n-1)}{4}\eta^4 + \dots \quad (18)$$

Keeping only zeroth and first order terms in η_k^2 , the inversion can be written, after some algebra, as

$$\begin{aligned}W(t) &= \cos(2\tilde{g}t) \mathcal{R}e \left(\prod_k \frac{1}{\bar{n}_k + 1 - \bar{n}_k e^{-i2\tilde{g}t\eta_k^2}} \right) \\ &- \sin(2\tilde{g}t) \mathcal{I}m \left(\prod_k \frac{1}{\bar{n}_k + 1 - \bar{n}_k e^{-i2\tilde{g}t\eta_k^2}} \right).\end{aligned} \quad (19)$$

In the following we use dimensionless variables such that the quantum dot-cavity coupling $g = 1$, but keep it in the formulas for clarity. There are some special cases worth studying separately.

A. Single phonon mode

In the simplest case consisting of a single phonon mode characterized by η and \bar{n} , the inversion (19) simplifies to

$$W(t) = \frac{(\bar{n} + 1) \cos(2\tilde{g}t) - \bar{n} \cos[2\tilde{g}t(1 - \eta^2)]}{(\bar{n} + 1)^2 + \bar{n}^2 - 2\bar{n}(\bar{n} + 1) \cos(2\tilde{g}t\eta^2)}. \quad (20)$$

The second term oscillates with a slightly shifted frequency causing a collapse of the inversion. When the two competing terms return back in phase, at times

$$t_{rev}^{(1)} = k \frac{\pi}{\tilde{g}\eta^2}, \quad k = 1, 2, 3, \dots, \quad (21)$$

inversion revivals occur. These are perfect within the small η^2 expansion. For short times t , the inversion may be further approximated to give

$$W(t) = \frac{\cos(2\tilde{g}t)}{1 + 8\bar{n}(\bar{n} + 1)\tilde{g}^2\eta^4t^2}, \quad 2\tilde{g}t\eta^2 \ll 1, \quad (22)$$

and we conclude that the envelope function, determining the collapse time, is a Lorentzian with width

$$t_{col}^{(1)} = \frac{1}{\sqrt{8\bar{n}(\bar{n} + 1)}\tilde{g}\eta^2}. \quad (23)$$

For larger values of η^2 , higher order terms in the expansion (18) must be included and perfect revivals are no longer present. Additionally, it is likely that the rotating wave approximation applied in eq. (6) breaks down for increasing η^2 . In fig. 1 we display three different examples of the atomic inversion (17), *i.e.* calculated from the RWA formula where the small η expansion has not been applied. The upper plot has a large average number of phonons; $\bar{n} = 40$, and $\eta = 0.1$ and it is clear that perfect revivals are lost due to large η . In the second plot the number of phonons are the same but $\eta = 0.02$ and the revivals are almost perfect. Note as well that the revival times are longer in this example. Finally in the last plot $\bar{n} = 2$ and $\eta = 0.01$ and we can conclude that a lower temperature of the reservoir increases the collapse time. These observations are in perfect agreement with the above derived approximations, and for figs. 1 (b) and (c) the expression (20) almost exactly agrees with the exact one. In the long time evolution of the system, the higher order terms of the Laguerre expansion (18) start to play an important role, and *fractional* and *super* revivals may occur [22].

B. N identical phonon modes

By studying several identical phonon modes one may see the effect of multi modes in a simple analytic way. For N identical modes ($\eta_k = \eta_{k'} |c_{n_k}| = |c_{n_{k'}}|$ for $n_k = n_{k'}$)

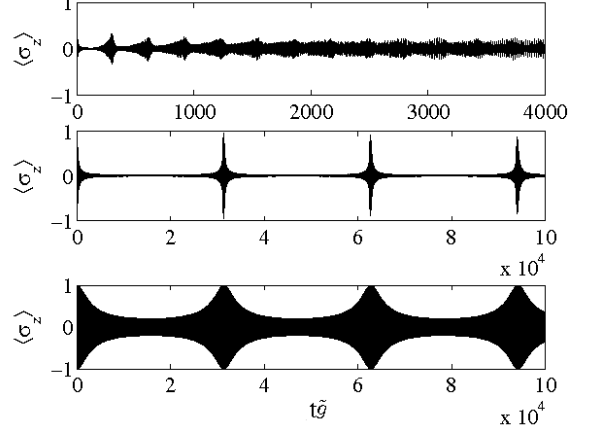


FIG. 1: The atomic inversion $W(t)$ as a function of time t for the single mode bath. The dimensionless parameters are $\eta = 0.1$ and $\bar{n} = 40$ for the upper plot, $\eta = 0.01$ and $\bar{n} = 40$ for the middle plot and $\eta = 0.01$ and $\bar{n} = 2$ for the lower plot.

of the phonon bath, the inversion (19) becomes

$$W(t) = \left[\frac{1}{(\bar{n} + 1)^2 + \bar{n}^2 - 2\bar{n}(\bar{n} + 1) \cos(2\tilde{g}t\eta^2)} \right]^N \times \sum_{j=0}^N \left\{ \binom{N}{j} (-\bar{n})^{N-j} (\bar{n} + 1)^j \times \cos[2\tilde{g}t(1 - (N - j)\eta^2)] \right\}. \quad (24)$$

Now the inversion is built up of several competing terms and the collapse will be more pronounced. This also follows directly from noting that the envelope function in this case is an identical Lorentzian as for the situation with a single mode, except that is is taken to the N th power. The collapse time can therefore be approximated by

$$t_{col}^{(N)} = \frac{(\sqrt[N]{2} - 1)^{1/2}}{\sqrt{8\bar{n}(\bar{n} + 1)}\tilde{g}\eta^2}. \quad (25)$$

Fractional revivals, hardly visible, take place at

$$t_{j,rev}^{(N)} = k \frac{\pi}{(N - j)\tilde{g}\eta^2}, \quad k = 1, 2, 3, \dots, \quad (26)$$

and for the perfect revivals we have $t_{rev}^{(N)} = t_{rev}^{(1)}$. Figure 2 shows the atomic inversion for different number of identical modes obtained from eq. (24) in (a) and from eq. (17) in (b). We note that the approximation breaks down when the number of phonon modes is increased; the revivals are no longer perfect and they occur earlier. The fact that the revival times are shorter is due to the higher order terms in the expansion (18), which becomes

more important for a large number of modes. Note, however, that η^2 is rather large in this example in order to see the effect.

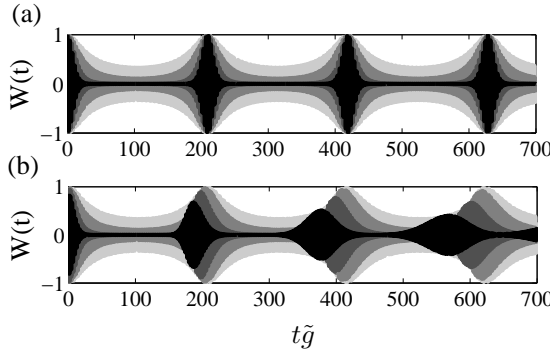


FIG. 2: The atomic inversion for 10 (black), 5 (dark gray), 4 (gray) and 1 (light gray) identical phonon modes. The upper plot (a) displays the results using the small η^2 expansion (24), and the lower (b) shows the exact (17). The parameters are $\bar{n} = 1$ and $\eta^2 = 0.015$.

C. N different phonon modes

In a more realistic model the phonon bath consists of non-identical modes, and depending on the model studied one has different spectral functions $J(\omega) = \sum_k \lambda_k^2 \delta(\omega - \omega_k)$ [23]. For the frequencies of interest here, $J(\omega)$ has a simple power law behaviour [24], resulting in a

$$\eta_k^2 = \kappa \omega_k^s, \quad s = \dots, -2, -1, 0, 1, 2, \dots, \quad (27)$$

where κ is a constant. The power s depends on matter properties, for example; *ohmic damping* $J(\omega) \propto \omega$, *phonon damping* $J(\omega) \propto \omega^3$ or *impurity damping* $J(\omega) \propto \omega^5$, but it also depends on system dimensions. We take $\omega_k = \omega_0 k$, $k = 1, 2, 3, \dots$ such that ω_0 determines the frequency spacing, while the thermal phonon distributions are determined from the average phonon numbers

$$\bar{n}_k = \left[\exp \left(\frac{\omega_k}{\tilde{T}} \right) - 1 \right]^{-1}, \quad (28)$$

for some scaled temperature \tilde{T} . Often a frequency “cut-off” is introduced for the spectral function, but because the vacuum modes do not affect the system dynamics in our case, such a cut-off is not needed. Defining $c_k = 8\bar{n}_k(\bar{n}_k + 1)\tilde{g}^2\eta_k^4$, and using the same arguments as above the collapse time in the small η^2 expansion is given by

$$\prod_k (1 + c_k t_{col}^2) = 2. \quad (29)$$

By further introducing

$$r_k = \sqrt{(\bar{n}_k + 1)^2 + \bar{n}_k^2 - 2\bar{n}_k(\bar{n}_k + 1)\cos(2\tilde{g}t\eta_k^2)},$$

$$\theta_k = \arctan \left[\frac{\bar{n}_k \sin(2\tilde{g}t\eta_k^2)}{\bar{n}_k + 1 - \bar{n}_k \cos(2\tilde{g}t\eta_k^2)} \right] \quad (30)$$

the approximated atomic inversion (19) can be written as

$$W(t) = \frac{\cos(2\tilde{g}t + \theta)}{r}, \quad (31)$$

where $\theta = \sum_k \theta_k$ and $r = \prod_k r_k$. In fig. 3, five examples of the atomic inversion in the small η^2 expansion are displayed for different powers s . Perfect revivals clearly occur for the $s = 0$, $s = 1$ and $s = 2$ cases, while for $s = -2$ and $s = -1$ the revivals are never fully perfect even at long times. This is because if $s = 0, 1, 2, \dots$ we have $\eta_k^2 = \kappa \omega_k^s = \kappa \omega_0^s k^s \equiv \eta_0^2 j$ where j is a positive integer, which does not hold if $s = \dots, -2, -1$. Note that the revivals are a consequence of the non Markovian treatment of the problem; the dynamics is unitary. Also when a large number of different phonon modes are coupled to the QD-cavity system revivals occur.

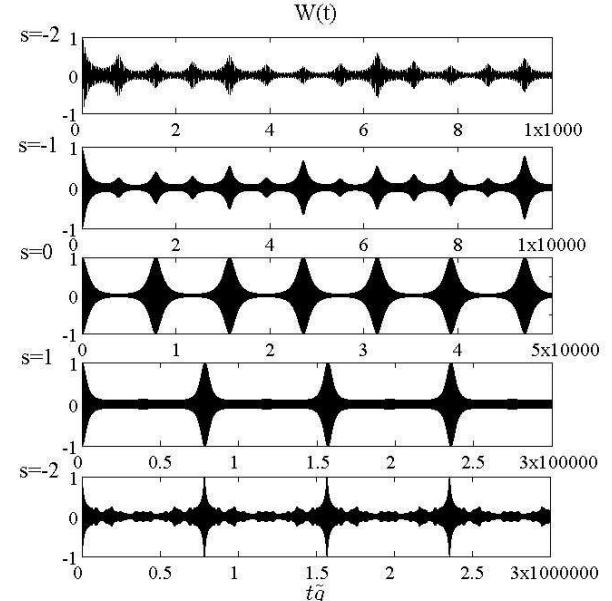


FIG. 3: Atomic inversion for different phonon modes obtained from the small η^2 expansion (19). The plots show respectively from top to bottom the cases with powers $s = -2, -1, 0, 1, 2$ of eq. (27). The other parameters are the same for all five cases; $T = 0.2$, $\kappa = 0.0004$ and $\omega_0 = 0.1$.

IV. BEYOND THE ROTATING WAVE APPROXIMATION

So far all the results have been derived or calculated within the RWA, which for $g\eta/\omega \ll 1$ is expected to be

justified. In this section we calculate the atomic inversion by numerically diagonalize the truncated Hamiltonian of eq. (5). The size of the Hamiltonian is chosen such that convergence of its eigenstates is guaranteed. We restrict the analysis to the one phonon mode case, which already explains most effects. In the Fock state basis $\{|m\rangle\}$ of the phonon mode, the matrix elements of the Hamiltonian are obtained by using the formula

$$D_{mn} \equiv \langle m | \hat{D}(\eta) | n \rangle = e^{-|\eta|^2/2} \eta^{n-m} \sqrt{\frac{m!}{n!}} L_m^{n-m}(|\eta|^2), \quad m \leq n, \quad (32)$$

where L_i^j is an associated Laguerre polynomial.

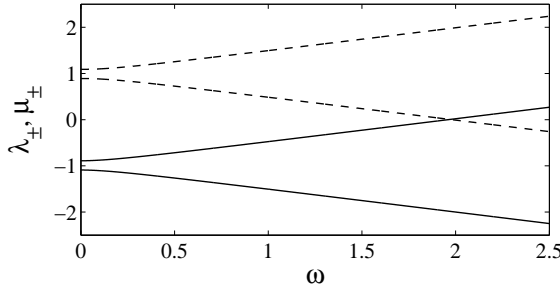


FIG. 4: The eigenvalues (34) as function of ω , with $\eta^2 = 0.01$. Dashed curves show μ_{\pm} and solid curves λ_{\pm} .

For lowest order truncation of the Hamiltonian, one keeps only a single Fock state of the phonon mode, and the results above where the RWA has been imposed are regained [28]. In this approximation, when the initial states of the phonon modes are on the form $|c_{n_k}\rangle = \delta_{n_k, n'_k}$, the combined quantum dot-cavity system persists perfect Rabi oscillations with a rescaled vacuum Rabi frequency $g \rightarrow \tilde{g} \prod_{n'_k} L_{n'_k}(\eta_{n_k}^2)$. For zero temperature, all the modes are in the vacuum and the above approximation simply gives a rescaled frequency $g \rightarrow \tilde{g}$, which is the result presented in [12]. Thus, this simple derivation regains the results of [12], and from it, it is also clear how the approximation comes about and easily extended to non-zero temperature phonon baths. A deeper insight of the approximation (RWA) is gained by increasing the size of the truncated Hamiltonian. In other words, to go beyond the RWA one needs to include more coupling terms arised due to the phonon bath. Considering an initial vacuum phonon mode and including first order corrections to the RWA, the Hamiltonian can be written in matrix form (after an overall shift in energy)

as

$$H_{vac} = \begin{bmatrix} -\frac{\omega}{2} & 0 & D_{00} & D_{01} \\ 0 & \frac{\omega}{2} & D_{01} & D_{11} \\ D_{00} & D_{01} & -\frac{\omega}{2} & 0 \\ D_{01} & D_{11} & 0 & \frac{\omega}{2} \end{bmatrix}, \quad (33)$$

with eigenvalues

$$\lambda_{\pm} = -\frac{D_{00} + D_{11}}{2} \pm \frac{1}{2} \sqrt{(D_{00} - D_{11} + \omega)^2 + 4D_{01}^2} \quad (34)$$

$$\mu_{\pm} = \frac{D_{00} + D_{11}}{2} \pm \frac{1}{2} \sqrt{(D_{00} - D_{11} - \omega)^2 + 4D_{01}^2}.$$

These eigenvalues are shown in fig. 4 as function of ω for fixed η ; λ_{\pm} (solid lines) and μ_{\pm} (dashed lines). The bare curves, $\epsilon_{\pm}^{\lambda} = -D_{ii} \pm \omega/2$ and $\epsilon_{\pm}^{\mu} = D_{ii} \pm \omega/2$, where $i = 0, 1$, are coupled by the non-RWA term D_{01} and the crossing at $\omega = 0$ is therefore *avoided*. Thus, in the RWA, the difference in the values D_{ii} for $i = 0, 1, 2, \dots$ of the bare energies at $\omega = 0$ causes the collapse-revival structure. However, as the non-RWA terms start to become important, the bare energies are no longer proportional to $\pm\omega$ and the dynamics will be modified. For which ω that this non linear behaviour occurs, depends, of course, on g and η . A rough estimate can be derived by assuming that the linear dependence of $\omega/2$ should dominate over the avoided crossing energy difference $2D_{01}$, which after expanding in η gives $\omega \gg 4g\eta$. In other words, using our typical parameter values, when $\omega < 1$ the RWA is likely to break down. For small ω , the eigen energies are very densely spaced, and a small non-RWA correction will couple the different energies in an involved way. The number of states taken into account to correctly describe the dynamics is then growing large, which is seen in fig. 5 showing the numerically obtained eigenvalues for a 12×12 dimensional (a) and a 22×22 dimensional (b) Hamiltonian. Clearly the more states taken into account, the more complicated energy spectrum.

In fig. 6 we give one example of the numerically obtained inversion in a regime where the RWA is not justified. Interestingly, for $\omega \ll 1$ the state $|g\rangle$ (opposite of the initial state) of the QD is more strongly populated, while for increasing ω the collapse revival pattern is clearly seen and $W(t) \rightarrow 1/2$ in the collapse regions.

V. CONCLUSIONS

We have studied a quantum dot strongly coupled to a single high-finesse optical cavity mode by applying methods usually applied in ion-laser interactions, namely the decomposition of the Glauber displacement operator in

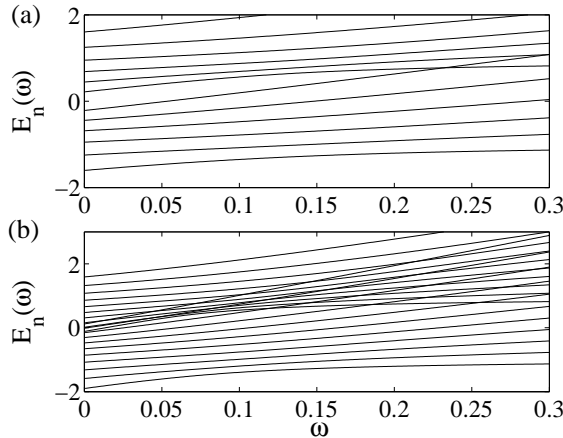


FIG. 5: The numerically obtained eigenvalues as function of ω , with $\eta^2 = 0.05$. In (a) the truncated Hamiltonian has size 12×12 and in (b) 22×22 . Due to the non-RWA coupling the curve crossings become avoided, which is, however, not seen in the plots of this size.

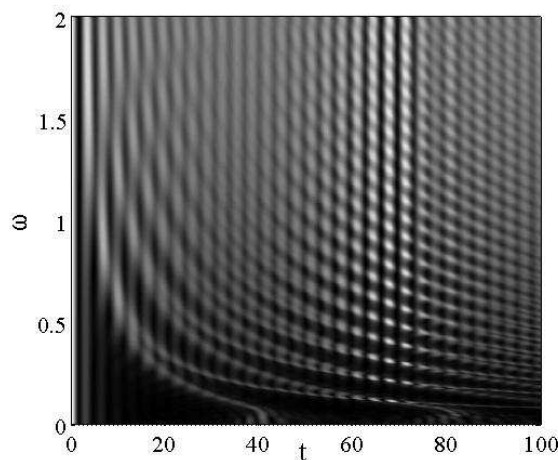


FIG. 6: The inversion as function of ω in the regime where the RWA breaks down. The revivals at $t_{rev} = \pi/\eta^2$ build up for increasing ω . Here $\eta^2 = 0.01$ and $\bar{n} = 3$.

Laguerre polynomials. This allowed us to obtain results for many phonon modes beyond the Born-Markov approximation. We have studied several cases, including N identical and N different phonon modes, i.e. the case of non-zero temperature. Analytical expressions for the collapse and revival times of the Rabi oscillations have been derived analytically, valid in a large range of parameters.

The analysis is carried out in the resonance condition $\Delta = \Delta_\eta$, which in the RWA gives that no population is transferred between the QD and the phonon reservoir. If this resonance is not fulfilled, but other specific types of conditions are (blue or red detuned), one may derive different types of effective Hamiltonians in the RWA, in

much resemblance with ion-trap cavity systems [3]. Then the effective models will be described by typical generalized two-mode Jaynes-Cummings Hamiltonians, which can often be solved analytically [27]. Another assumption made in the derivation is that the cavity mode is initially in vacuum, while for a general initial state each photon states will, just like in the case of the various phonon states, induce different Rabi frequencies affecting the collapse-revival pattern. Such situation may be of interest for state preparation or state measurement and is left for future considerations.

We have also presented a short analysis of the non RWA regime. In this regime, the energy spectrum becomes very complex with crossing energy curves, and as the energy spacing between the curves is small for these parameters many eigenstates of the Hamiltonian must be included in order to correctly describe the dynamics. Non the less, from such an approach it is seen how the RWA results are gained as a first order correction to the trivial situation, and how higher order terms cause avoided crossings between the energies, and they are therefore no longer proportional to $\pm\omega$ that will induce a “break-down” of the collapse-revival pattern. The higher order terms in such an expansion can be seen as a virtual exchange of phonons [28].

Acknowledgments

This work was supported by EU-IP Programme SCALA (Contract No. 015714), the Swedish Government/Vetenskapsrådet and Consejo Nacional de Ciencia y Tecnología.

[1] A. Imamoglu, D. D. Awschalom, G. Burkard, D. P. Di-Vincenzo, D. Loss, M. Sherwin, and A. Small, Phys. Rev. Lett. **83**, 4204 (1999); A. Miranowicz, . K. zdemir1, Y. Liu, Masato Koashi, N. Imoto1, and Y. Hirayama1, Phys. Rev. A **65**, 062321 (2002); M. Feng, I. D'Amico, P. Zanardi, and F. Rossi, Phys. Rev. A **67**, 014306 (2003); X. Wang, M. Feng and B.C. Sanders, Phys. Rev. A **67**, 022302 (2003).

[2] J. M. Gérard, B. Sermage, B. Gayral, B. Legrand, E. Costard, and V. Thierry-Mieg, Phys. Rev. Lett. **81**, 1110 (1998); C. Becher1, A. Kiraz1, P. Michler1, A. Imamolul, W. V. Schoenfeld, P. M. Petroff, Lidong Zhang, and E. Hu, Phys. Rev. B **63**, 121312 (2001); A. Kiraz, C. Reese, B. Gayral, L. Zhang, W.V. Schoenfeld, B.D. Gerardot, P.M. Petroff, E.L. Hu, and A. Imamoglu, J. Opt. B **5**, 129 (2003).

[3] B.W. Shore and P.L. Knight, J. Mod. Optics **40** 1195 (1993).

[4] M. Brune, S. Haroche, J. M. Raimond, L. Davidovich, and N. Zugary, Phys. Rev. A **45**, 5193 (1992); M. Brune, E. Hagley, J. Dreyer, X. Maitre, A. Maali, C. Wunderlich, J. M. Raimond, and S. Haroche, Phys. Rev. Lett. **77**, 4887 (1996); S. Brattke, B. T. H. Varcoe, and H. Walther, Phys. Rev. Lett. **86**, 3534 (2001).

[5] J. M. Raimond, M. Brune, and S. Haroche, Rev. Mod. Phys. **73**, 565 (2001).

[6] D. Leibfried, R. Blatt, C. Monroe, and D. Wineland, Rev. Mod. Phys. **75**, 281 (2003).

[7] D. Kielpinski, C. Monroe, and D. J. Wineland, Nature **417**, 709 (2002).

[8] D. Leibfried, D. M. Meekhof, C. Monroe, B. E. King, W. M. Itano, and D. J. Wineland, J. Mod Opt. **44**, 2485 (1997); C. Roos, T. Zeiger, H. Rohde, H. C. Nagerl, J. Eschner, D. Leibfried, F. Schmidt-Kaler, and R. Blatt, Phys. Rev. Lett. **83**, 4713 (1999).

[9] A. Wallraff, D. I. Schuster, A. Blais, L. Frunzio, R. S. Huang, J. Majer, S. Kumar, S. M. Girvin, R. J. Schoelkopf, Nature **431**, 162 (2004); D. I. Schuster, A. A. Houck, J. A. Schreier, A. Wallraff, J. M Gambetta, A. Blaise, L. Frunzio, J. Majer, B. Johnson, M. H. Devoret, S. M. Girvin, R. J. Schoelkppf, Nature **445**, 515 (2007).

[10] A. Wuergler, Phys. Rev. B **57**, 347 (1998).

[11] I. Wilson-Rae and A. Imamoglu, Phys. Rev. B **65**, 235311 (2002).

[12] L. Wai-Sang, and Z. Ka-Di, Chin. Phys. Lett. **20**, 1568 (2003); Z. Ka-Da, and L. Wai-Sang, Phys. Lett. A **314**, 380 (2003).

[13] H. -P. Breuer, and F. Petruccione, *The theory of open quantum systems*, (Oxford University Press, 2003); C. W. Gardiner, and P. Zoller, *Quantum Noise*, (Springer Verlag, 2004).

[14] Ka-Di Chin, Z-J. Wu, X-Z. Yuan, and H. Zheng, Phys. Rev. B **71**, 235312 (2005).

[15] C.B. Duke and G.D. Mahan, Phys. Rev. **139**, A1965 (1965).

[16] D. Leibfried, R. Blatt, C. Monroe, and D. Wineland, Reviews of Modern Physics **75**, 281 (2003).

[17] S. Wallentowitz, W. Vogel and P.L. Knight, Phys. Rev. A **59** 531 (1999); S. Wallentowitz adn W. Vogel, Phys. Rev. A **58** 679 (1998).

[18] K. Huang, and A. Rhys, Proc. R. Soc. Lond. A **204**, 406 (1950).

[19] R. Heitz, I. Mukhametzhanov, O. Stier, A. Madhukar, and D. Bimberg, Phys. Rev. Lett. **83**, 4654 (1999).

[20] T. H. Stievater, X. Li1, D. G. Steel, D. Gammon, D. S. Katzer, D. Park, C. Piermarocchi, and L. J. Sham, Phys. Rev. Lett. **87**, 133603 (2001); H. Kamada, H. Gotoh, J. Temmyo, T. Takagahara, and H. Ando, Phys. Rev. Lett. **87**, 246401 (2001).

[21] V. Turck, S. Rodt, O. Stier, R. Heitz, R. Engelhardt, U. W. Pohl, D. Bimberg, and R. Steingruber, Phys. Rev. B **61**, 9944 (2000).

[22] M. V. Satyanarayana, P. Rice, R. Vyas, and H. J. Carmichel, J. Opt. Soc. Am. B **6**, 228 (1989); S. S. Averbukh, Phys. Rev. A 46, R2205 (1992); P. F. Gra, and C. Jedrzejek, Phys. Rev. A **48**, 3291 (1993).

[23] G. D. Mahan, *Many-Particle Physics*, (Kluwer, new York 2000).

[24] A. J. Leggett, S. Chakravarty, A. T. Dorsey, M. P. A. Fisher, A. Garg, and W. Zwerger, Rev. Mod. Phys. **59**, 1 (1987).

[25] J. Larson, and H. Moya-Cessa, J. Mod. Opt. **??**, **??** (2007).

[26] V. Buzek, G. Drogny, M. S. Kim, G. Adam, and P. L. Knight, Phys. Rev. A **56**, 2352 (1997).

[27] B. W. Shore, and P. L. Knight, J. Mod. Opt. **40**, 1195 (1993); A. Messina, S. Maniscalco, and A. napoli, J. Mod. Opt. **50**, 1 (2003).

[28] J. Larson, J. Salo, and S. Stenholm, Phys. Rev. A **72**, 013814 (2005).